PROCEEDINGS OF SCIENCE

Hunting Neutrino Sources in our Galaxy: The Most Promising Targets associated with Supernova Remnants

Ryan Burley,[a,*] **Sabrina Einecke,**[a] **Gavin Rowell,**[a] **Gary Hill**[a] **and Jenni Adams**[b]

[a] *School of Physics, Chemistry and Earth Sciences, The University of Adelaide, Adelaide, 5005, Australia*

[b] *Department of Physics and Astronomy, University of Canterbury, Private Bag 4800, Christchurch, New Zealand*

E-mail: ryan.burley@adelaide.edu.au

To this date, the existence and locations of high-energy neutrino sources in our Galaxy are a big mystery. Their identification would be a smoking gun signature for a hadronic cosmic-ray accelerator, providing vital information to shed light on the origin of Galactic cosmic rays and the properties of Galactic PeVatrons. High-energy gamma rays and neutrinos can both be produced by the decay of mesons that are created in inelastic collisions of cosmic rays and the interstellar gas. This correlation would also allow us to decipher the fraction of gamma rays produced by electrons. In this contribution, we will introduce and discuss the most promising supernova remnants and molecular gas clouds to hunt for Galactic neutrino sources and PeVatrons. We will introduce our novel 3D modelling of cosmic rays escaping supernova remnants to interact with nearby molecular gas clouds. We will discuss how we determine the most promising targets to be detected by the IceCube Neutrino Observatory and the Cherenkov Telescope Array, and how these targets vary under a range of system parameters, such as the gas and supernova remnant properties.

38th International Cosmic Ray Conference (ICRC2023)
26 July - 3 August, 2023
Nagoya, Japan

ICRC2023
38th International Cosmic Ray Conference
The Astroparticle Physics Conference

*Speaker

PoS(ICRC2023)1176

1. Introduction

The origin of Galactic cosmic rays remains a primary open problem in astroparticle physics, even after a century of research. It has long been proposed that supernova remnants (SNRs) provide suitable environments to accelerate charged particles to PeV energies. These energies coincide with the 'knee' observed in the cosmic-ray spectrum (≈3 PeV), which likely indicates the maximum energy that particles are accelerated to within the Galaxy. Depending on the charged particles' energy, they can escape the shock front of their SNR to diffuse into the surrounding interstellar medium and interact with the environment. The hadronic interactions that occur result in pion decay which produce high-energy neutrinos and gamma rays, which may be detectable from Earth. Observing these particles provides evidence for the acceleration of high-energy charged particles, while revealing other important information about the nature of these accelerators. Notably, the joint observation of neutrinos and gamma rays can discriminate between the hadronic and leptonic nature of an accelerator. Previous studies have looked into neutrinos and gamma rays due to hadronic interactions between SNRs and nearby molecular clouds (MCs), and the feasibility of detecting these particles [1–5]. Such combinations may be responsible for unresolved sources of gamma rays observed by H.E.S.S. [6] and LHAASO [7], or some contribution of the recently revealed diffuse Galactic plane neutrino flux reported by IceCube [8].

In this contribution, we present our extension on the work of [3] to also consider the flux of neutrinos expected from SNR and MC combinations. We advance on this idea by undertaking a new 3D modelling of both the protons and the ISM to obtain particle fluxes using the software presented in [9], including a revised treatment of the proton diffusion length. We also further simulate the response of the upcoming Cherenkov Telescope Array to these extended gamma-ray sources to identify promising SNR/MC pairs, and their associated neutrino flux. We present a preliminary look at how the IceCube Neutrino Observatory would see our most optimistic SNR/MC combinations.

2. Modelling Proton Distribution and Particle Production

2.1 Cosmic-ray Protons

The following methodology is mostly implemented within a newly developed software capable of modelling the transport of cosmic rays in three dimensions and their hadronic and leptonic interactions in the surrounding environment [9]. We consider the analytical solution of the diffusive transport equation from [1] for an impulsive source with a power-law injection spectrum of index α. This solution describes the proton density surrounding an SNR, J_p, of protons with energy E_p that have diffused a distance R from the SNR after time t has elapsed since the supernova explosion, after escaping the SNR with radius R_esc at time t_esc. This is given by:

$$J(E_\mathrm{p}, R, t) = \frac{N_0\, E_\mathrm{p}^{-\alpha}\, f_0}{\pi^{3/2} R_\mathrm{d}(E_\mathrm{p})^3} \exp\left[-\frac{(R - R_\mathrm{esc})^2}{R_\mathrm{d}(E_\mathrm{p})^2}\right] \exp\left[-\frac{(\alpha - 1)(t - t_\mathrm{esc})}{\tau_\mathrm{pp}(E_\mathrm{p})}\right], \tag{1}$$

where the constant, N_0, is normalised so the energy budget available for cosmic rays from the supernova, W_p, is spread across the minimum and maximum energy of particles present at the Sedov time, $E_\mathrm{p,min}$ and $E_\mathrm{p,max}$, respectively. For a given remnant, $W_\mathrm{p} = \eta E_\mathrm{SN}$, where E_SN is the total kinetic energy of the precursor supernova explosion and η is the cosmic-ray acceleration efficiency

of the SNR. Considering that the proton lifetime $\tau_{pp}(E_p) \ll t$ in a low-density environment, we can adopt a simplified energy-dependent diffusion length, R_d, where $R_d(E_p) = \sqrt{4D(E_p)(t - t_{esc})}$. Here $D(E_p)$ is the diffusion coefficient and is given as [4]:

$$D(E_p) = \chi D_0 \left(\frac{E_p/\mathrm{GeV}}{B/3\mu\mathrm{G}} \right)^{\delta}, \tag{2}$$

with diffusion-suppression coefficient χ, reference diffusion coefficient at 1 GeV, D_0 ($3 \times 10^{-27} \mathrm{cm}^{-2}\,\mathrm{s}^{-1}$), magnetic field B (we use Equation 21 in [32] for B in a MC, and 3μG in the interstellar medium [33]), and diffusion index δ. To account for the difference in diffusion a proton experiences in the ISM to that in the MC, we consider a differential approach to obtain an effective diffusion length value to satisfy the single diffusion. By rearranging the expression for $R_d(E_p)$ and differentiating with respect to time, we get an expression for a proton travelling incremental distances in steps of time. By then translating these distance steps to regions of the ISM and the MC and considering their respective diffusion properties, we can sum the steps in time until they equal the time since the proton escaped the SNR. The associated distance is used as an effective differential length in the consequent modelling. The factor, f_0, was adapted in [3] to account for the energy-dependent release of protons from a SNR shock expanding with time as:

$$f_0 = \frac{\sqrt{\pi} R_d(E_p)^3}{(\sqrt{\pi} R_d(E_p)^2 + 2\sqrt{\pi} R_{SNR}(t)^2) R_d(E_p) + 4 R_{SNR}(t) R_d(E_p)^2}. \tag{3}$$

The time-dependent SNR radius in the Sedov-Taylor phase of expansion, $R_{SNR}(t)$ is found with Equation 52 in [22] for an upstream density of n_0 ($1\,\mathrm{cm}^{-3}$ used in this work) and mean mass per hydrogen atom μ_H of 1.4. The escape time is described by [23]:

$$t_{esc}(E_p) = t_{sedov} \left(\frac{E_p}{E_{p,max}} \right)^{-1/\beta}, \tag{4}$$

where t_{sedov} is the Sedov time (indicating the age at which the SNR enters the Sedov-Taylor stage) and β describes the temporal evolution of the magnetic turbulence (where $\beta = 2.5$). In this work, the Sedov time, dependent on E_{SN}, ejecta mass M_{ej}, and n_0, is calculated according to [24]. The respective R_{esc} can be obtained by inputting t_{esc} into the aforementioned equation in [22].

2.2 Neutrino and Gamma-ray Production

The flux of neutrinos and gamma rays is calculated by considering the interactions of the protons with some target material. For brevity going forward, the use of neutrinos in this text refers to both the neutrinos and anti-neutrinos of a given flavour produced in some interaction. The flux at Earth, $\mathrm{d}N_j(E_j)/\mathrm{d}E_j$, of particles in the energy range $(E_j, E_j + dE_j)$, where j refers to either gamma rays (γ) or neutrinos (ν), arriving from volume V containing density n, is found with:

$$\frac{\mathrm{d}N_j(E_j)}{\mathrm{d}E_j} = \frac{c\, n\, V}{4\pi D^2} \int_{E_j}^{\infty} \sigma_{inel}(E_p)\, J(E_p, R, t)\, F_j\left(\frac{E_j}{E_p}, E_p\right) \frac{dE_p}{E_p}, \tag{5}$$

with speed of light c, particles produced per particle collision $F_j(E_j)$ (listed in [14]), and proton-proton inelastic cross section $\sigma_{inel}(E_p)$ (we use the parameterisation in [19]).

While neutrinos travel mostly uninhibited, gamma rays produced in these environments would be subject to pair absorption with interstellar radiation fields (ISRFs) as they travel to Earth. To account for this reduction in flux, we adapt each photon flux following the description in [20], using the ISRF model developed in [21]. The pair absorption optical depth values required to perform these calculations were obtained from the GALPROP website[1]. As neutrinos propagate, they oscillate between their three flavours. We approximate that for neutrinos travelling Galactic distances, they oscillate from a (ν_e:ν_μ:ν_τ) flavour ratio of (1:2:0) at the source to (1:1:1) at Earth [25].

3. Supernova Remnant and Molecular Cloud Combinations

The SNRs considered in this analysis are the 303 SNRs listed in the latest Green catalogue of Galactic supernova remnants[2] [10]. Coordinates and angular size of each SNR were obtained from this catalogue, while distance measures and age estimates, where available, were obtained from SNRcat[3] [11]. The Galactic molecular clouds used in this work are the 1064 presented in the catalogue from [12]. These clouds cover a Galactic longitude of $13° < l < 348°$ and Galactic latitude $|b| < 1°$, and were identified in the all-Galaxy CO survey, presented in [13]. As the distance for a cloud is inferred using a measure of gas velocity, many clouds have two possible distance values due to the ambiguity in the Galactic rotation model solution. As such, each distance estimate carries a unique cloud mass and physical size estimate, which are used to determine the number density n of a cloud.

An extensive number of SNR/MC combinations arise from combining these catalogues, which increases when including both distance measures for clouds. Rather than simulating all pairs, criteria are applied to remove irrelevant combinations and reserve computation time for the most promising candidates. As in [3], combinations are only considered if there is less than 100 pc between the closest point of separation of the SNR and accompanying MC, which requires knowledge of the distance and sizes of both objects. As there are large uncertainties for the MC and SNR distances (if available), we consider optimistic limits to find promising candidates. For SNRs with a distance estimate in [11], if a MC has a distance within the SNR distance range, the SNR is placed at the MC distance. For SNRs without a distance measure, it is placed at the same distance as the MC. For SNRs with an age estimate, their radius is obtained from the time-dependent radius in [22], otherwise a radius estimate is obtained by combining the angular radius of the SNR in [10] and the distance to the accompanying MC.

Each MC is treated as a sphere based on the cloud radius provided in [12]. When modelling a MC, it is deconstructed into cubes of 1 pc sides, each containing n of that cloud. In any case where the spheres of the SNR and MC overlap, the SNR is moved such that there is 1 pc between the objects, with SNRs within MCs planned to be considered in future work. Another initial check determines whether the combination produces a gamma-ray flux at 100 TeV greater than $1\times10^{-18}\,\mathrm{TeV^{-1}cm^{-2}s^{-1}}$, as preliminary work found such combinations did not produce a significant gamma-ray flux for energies greater than 100 TeV.

[1] https://galprop.stanford.edu

[2] Green D. A., 2022, *'A Catalogue of Galactic Supernova Remnants (2022 December version)'*, Cavendish Laboratory, Cambridge, United Kingdom (available at http://www.mrao.cam.ac.uk/surveys/snrs/)

[3] http://www.physics.umanitoba.ca/snr/SNRcat

Model Parameter	Values
χ	0.1, 0.01, 0.001
δ	0.3, 0.5
η	0.1, 0.3
$E_{\mathrm{p,max}}$	1 PeV, 5 PeV
α	2, 2.2
E_{SN}, M_{ej}	(10^{51} erg, 1.4 $\mathrm{M}_{\odot}$), (10^{51} erg, 10 $\mathrm{M}_{\odot}$), (10^{52} erg, 20 $\mathrm{M}_{\odot}$)

Table 1: Model parameters varied across simulations and the accompanying values used. Parameter descriptions are provided in Section 2. A total of 144 unique parameter sets are considered in this work for each SNR/MC combination, which are performed for a range of SNR ages and distances, dependent on the literature in [11].

Following this setup, we obtain the neutrino and gamma-ray fluxes that result from a range of unique model parameters sets for every SNR/MC pair. Each combination has a range of SNR age and distances considered, proportional to the amount of literature summarised in [11] for that SNR. To encapsulate the uncertainty of many of the model parameters described in Section 2, we consider an assortment of values for every SNR/MC combination, summarised in Table 1. This results in 144 unique model parameter sets simulated for every SNR/MC pair at each distance and age for that pair. Applying the above criteria, a total of $\approx 7.5\times10^{6}$ simulations were performed for 3,166 unique SNR/MC combinations.

4. Determining Promising Combinations

To quantify which SNR/MC combinations are most promising to observe, we first exclude combinations that produce a gamma-ray flux at 1 TeV exceeding that reported in the H.E.S.S. Galactic plane survey at the cloud position (assuming a power-law spectrum for the differential flux with index $\Gamma = 2.3$) [6]. We also exclude combinations which result in a gamma-ray flux at 100 TeV greater than the dimmest object observed by LHAASO, of 0.4 CU (where 1 CU = 6.1×10^{-17} photons $\mathrm{TeV}^{-1}\mathrm{cm}^{-2}\mathrm{s}^{-1}$) [7]. The flux from both instruments is scaled to each cloud size with Equation 15 from [3], where point spread functions of 0.2° and 0.3° are used for H.E.S.S. and LHAASO, respectively. In lieu of ≈100 TeV gamma-ray observations across the full Southern sky, we apply the same LHAASO limit across the entire sky to remove combinations with unreasonably large flux estimates in this region. We classify that the most promising combinations are those that produce a gamma-ray flux above 100 TeV that would be detectable with the Cherenkov Telescope Array at the southern site over 50 hours with a minimum significance of 5σ, at either a zenith angle of 40° or 60°. The calculations are performed using `gammapy` and the CTA instrument response functions provided in [26], with the significance calculated using Equation 17 from [27] with an acceptance ratio of 0.2.

The number of neutrinos events, N_ν, detected at the IceCube Neutrino Observatory from the region subtended by a MC can be found with:

$$N_\nu = \int_0^t dt \int_0^{R_{\mathrm{ang}}} d\Omega \int_{E_{\nu,\mathrm{min}}}^{E_{\nu,\mathrm{max}}} dE_\nu \, A_{\mathrm{eff}}(E_\nu, \delta) \, \frac{\mathrm{d}N_\nu(E_\nu)}{\mathrm{d}E_\nu}, \tag{6}$$

Median Property	SNR/MC combinations ($E_{p,\mathrm{max}}$ = 1 PeV)	SNR/MC combinations ($E_{p,\mathrm{max}}$ = 5 PeV)
SNR age (kyr)	5.0	4.5
MC number density (cm^{-3})	162.5	103.5
SNR-MC separation (pc)	83.8	94.0
Track event probability	2.1×10^{-3}	7.6×10^{-3}
Cascade event probability	6.1×10^{-3}	1.6×10^{-2}
CTA significance (σ)	5.3	5.5

Table 2: A selection of median values from the SNR/MC combinations which produce the largest predicted significance at the Cherenkov Telescope Array. The probability for track and cascade events is a basic measure to indicate the strength of the SNR/MC combination to the background, which is unsurprisingly stronger for SNRs with larger maximum energy protons.

with total observation time t, angular radius of the MC R_{ang}, energy and declination-dependent effective area of the detector $A_{\mathrm{eff}}(E_\nu, \delta)$ ([17] for track events and [18] for cascade events), and minimum and maximum neutrino energies, $E_{\nu,\mathrm{min}}$ and $E_{\nu,\mathrm{max}}$, respectively. All neutrino events are integrated from a minimum of 100 TeV to a maximum of the relevant $E_{\mathrm{p,max}}$, to consider a region where the astrophysical signal is less contaminated by the atmospheric background. We calculate three sets of neutrino events for each SNR/MC combination to understand the strength of the simulated neutrinos to the background. This is performed for both track events (muon neutrinos undergoing charged current interactions) and cascade events (all-flavour neutral current interactions and primarily electron and tau neutrino charged current interactions). The first set are neutrino events from the SNR/MC combination, $N_{\nu,\mathrm{cloud}}$, which uses the flux obtained following Section 2. The second set, $N_{\nu,\mathrm{diffuse}}$, are from the diffuse flux of astrophysical neutrinos, using [16] for muon neutrinos and [30] for electron and tau neutrinos. The final set, $N_{\nu,\mathrm{atmos}}$, are atmospheric neutrinos produced due to cosmic-ray interactions in the Earth's atmosphere. Here, the zenith-dependent atmospheric flux containing both conventional and prompt neutrinos is obtained using MCEq [15], where the *Gaisser-H4a* [28] primary cosmic-ray flux model and *Sibyll2.3c* [29] hadronic interaction models are configured. A simple neutrino probability measure of $N_{\nu,\mathrm{cloud}}$ / ($N_{\nu,\mathrm{cloud}}$ + $N_{\nu,\mathrm{diffuse}}$ + $N_{\nu,\mathrm{atmos}}$) quantifies here how a SNR/MC combination would appear compared to the background.

5. Results

A full picture of these results will be presented in a future publication, while here we present a selection of interesting results. For each unique SNR/MC combination, we select the set of parameters that results in the largest CTA-S significance. The following statistics for these top combinations are split between parameter sets with $E_{\mathrm{p,max}}$ = 1 and 5 PeV, to avoid biasing all results towards the 5 PeV simulations, which produce larger neutrino and gamma-ray fluxes by construction. A selection of descriptive statistics are listed in Table 2.

An example of the particle spectra that are obtained for a SNR/MC combination, SNR G106.3+02.7 and cloud #630 from [12], is shown in Figure 1. This particular SNR and cloud combination was chosen due to G106.3+02.7's status as a potential hadronic PeVatron [31], and shows how variations in the model parameters (while keeping $E_{\mathrm{p,max}}$ = 1 PeV) can significantly change the resulting particle spectra.

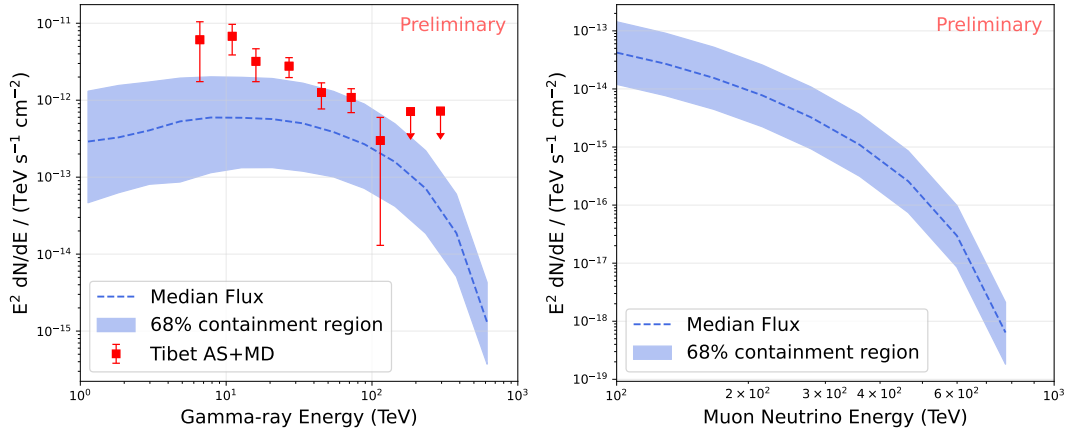

Figure 1: Energy spectra distribution for gamma rays (*left*) and muon neutrinos (*right*) of SNR G106.3+02.7 and cloud #630 from [12]. A total of 520 simulations each with unique model parameters were performed for this combination. The median flux for each particle is shown with a banded region containing 68% of the simulated energy spectra, indicating how varying parameters can greatly affect the resulting spectrum. The spectral points for the Tibet air shower array's observation of G106.3+02.7 [31] is shown, suggesting that some combination of the simulated parameters may explain the observed energy spectrum.

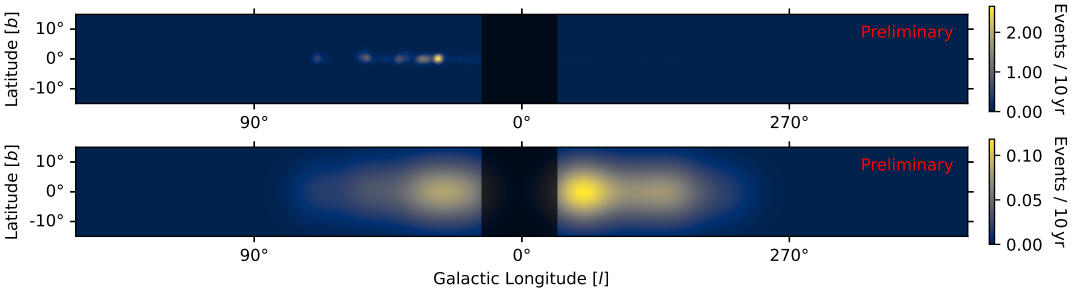

Figure 2: Event map distributions showing how IceCube would view track (*top*) and cascade (*bottom*) events from our most optimistic SNR/MC combinations over 10 years of observation. The track and cascade events have been smoothed for 1° and 10° angular resolutions, respectively. The banded region indicates the longitude range where [12] does not provide MCs. A pixel size of 0.3° by 0.3° is used.

For every top SNR/MC combination where $E_{\mathrm{p,max}} = 1$ PeV, Figure 2 shows how IceCube would view the neutrinos via both track and cascade events over 10 years. In both cases, the maps are convolved with 2D Gaussian distributions to take into account the 1° and 10° angular resolution of tracks and cascades, respectively. While only qualitative results are made here, it can be seen that neutrinos visible in these maps do align with regions of excess neutrino significance reported in [8].

This extensive, systematic study provides an exciting first look at how hadronic interactions between cosmic rays accelerated by supernova remnants and nearby molecular gas clouds could contribute to the recently revealed diffuse neutrino flux from the Galactic plane. Joint observation of neutrinos and gamma rays from these accelerators are key to understanding their nature, exhibiting why future instruments like the Cherenkov Telescope Array are vital to advancing our knowledge. A full description of these results and their implications will be presented in a future publication.

Acknowledgments

R.B. acknowledges the financial support of the Astronomical Society of Australia and the Walter and Dorothy Duncan Trust, which facilitated their attendance at this conference. This work was supported with supercomputing resources provided by the Phoenix HPC service at the University of Adelaide. This research has made use of the CTA instrument response functions provided by the CTA Consortium and Observatory, see https://www.ctao-observatory.org/science/cta-performance/ (version prod5 v0.1; [26]) for more details. This work made use of Astropy[4], a community-developed core Python package and an ecosystem of tools and resources for astronomy. This research made use of gammapy[5], a community-developed core Python package for TeV gamma-ray astronomy.

References

[1] F.A. Aharonian and A.M. Atoyan, *Astron. Astrophys.* **309** (1996) 917
[2] Y. Ohira, K. Murase and R. Yamazaki, *Mon. Not. R. Astron Soc.* **410** (2010) 1577
[3] A.M.W. Mitchell, G.P. Rowell, S, Celli and S. Einecke, *Mon. Not. R. Astron Soc.* **503** (2021) 3522
[4] S. Gabici, F.A. Aharonian and P. Blasi, *Astrophys. Space Sci.* **309** (2007) 365
[5] S. Gabici and F.A. Aharonian, *Astrophys. J. Lett.* **665** (2007) L131
[6] H.E.S.S. Collaboration et al., *Astron. Astrophys.* **612** (2018) A1
[7] Z. Cao et al., *Nature* **594** (2021) 33
[8] IceCube Collaboration et al., *Science* **380** (2023) 1338
[9] S. Einecke, G. Rowell, R. Burley, R. König, T. Collins and F. Voisin, *Modelling the Transport of Particles in the Interstellar Medium*, in proceedings of *38th International Cosmic Ray Conference*, PoS(ICRC2023)925 (2023)
[10] D.A. Green, *J. Astrophys. Astron.* **40** (2019) 36
[11] G. Ferrand and S. Safi-Harb, *Adv. Space Res.* **49** (2012) 1313
[12] T.S. Rice, A.A. Goodman, E.A. Bergin, C. Beaumont and T.M. Dame, *Astrophys. J.* **822** (2016) 52
[13] T.M. Dame, D. Hartmann and P. Thaddeus, *Astrophys. J.* **547** (2001) 792
[14] S.R. Kelner, F.A. Aharonian and V.V. Bugayov, *Phys. Rev. D* **74** (2006) 034018
[15] A. Fedynitch, R. Engel, T.K. Gaisser, F. Riehn and T. Stanev, *EPJ Web of Conferences* **99** (2015) 08001
[16] IceCube Collaboration et al., *Astrophys. J.* **928** (2022) 50
[17] IceCube Collaboration et al., *IceCube Data for Neutrino Point-Source Searches Years 2008-2018*, *arXiv:2101.09836* 10.21234/sxvs-mt83
[18] IceCube Collaboration et al., *Observation of high-energy neutrinos from the Galactic plane – Public data release*, 10.21234/8v5d-rn16
[19] E. Kafexhiu, F. Aharonian, A.M. Taylor and G.S. Vila, *Phys. Rev. D* **90** (2014) 123014
[20] T.A. Porter, G.P. Rowell, G. Jóhannesson and I.V. Moskalenko, *Phys. Rev. D* **98** (2018) 041302
[21] T.P. Robitaille, E. Churchwell, R.A. Benjamin, B.A. Whitney, K. Wood, B.L. Babler and M.R. Meade, *Astron. Astrophys.* **545** (2012) A39
[22] J.K. Truelove and C.F. McKee, *Astrophys. J. Suppl. Ser.* **120** (1999) 299
[23] S. Gabici, F.A. Aharonian and S. Casanova, *Mon. Not. R. Astron Soc.* **396** (2009) 1629
[24] S. Celli, G. Morlino, S. Gabici and F.A. Aharonian, *Mon. Not. R. Astron Soc.* **490** (2019) 4317
[25] M. Ahlers, Y. Bai, V. Barger and R. Lu, *Phys. Rev. D* **93** (2016) 013009
[26] Cherenkov Telescope Array Observatory and Cherenkov Telescope Array Consortium, *CTAO Instrument Response Functions - prod5 version v0.1*, 10.5281/zenodo.5499840
[27] T.P. Li and Y.Q. Ma, *Astrophys. J.* **272** (1983) 317
[28] T.K. Gaisser, *Astropart. Phys.* **35** (2012) 801
[29] A. Fedynitch, F. Riehn, R. Engel, T.K. Gaisser and T. Stanev, *Phys. Rev. D* **100** (2019) 103018
[30] IceCube Collaboration et al., *Phys. Rev. Lett.* **125** (2020) 121104
[31] The Tibet ASγ Collaboration et al., *Nat. Astron.* **5** (2021) 460
[32] R.M. Crutcher, B. Wandelt, C. Heiles, E. Falgarone and T.H. Troland, *Astrophys. J.* **725** (2010) 466
[33] R. Jansson and G.R. Farrar, *Astrophys. J.* **757** (2012) 14

[4] http://www.astropy.org
[5] https://www.gammapy.org